NEOPLASIA
www.neoplasia.com

Volume 14 Number 4 April 2012 pp. 335–343 335

Targeted Antivascular Therapy with the Apolipoprotein(a) Kringle V, rhLK8, Inhibits the Growth and Metastasis of Human Prostate Cancer in an Orthotopic Nude Mouse Model[1]

Ho-Jeong Lee[*,†], Hyun-Kyung Yu[*], John N. Papadopoulos[‡], Seung Wook Kim[‡], Junqin He[‡], Yong-Keun Park[†], Yeup Yoon[*], Jang-Seong Kim[*] and Sun Jin Kim[‡]

*Cancer Biology Team, Mogam Biotechnology Research Institute, Yongin, Republic of Korea; [†]School of Life Sciences and Biotechnology, Korea University, Seoul, Republic of Korea; [‡]Department of Cancer Biology, The University of Texas MD Anderson Cancer Center, Houston, TX, USA

Abstract

Antivascular therapy has emerged as a rational strategy to improve the treatment of androgen-independent prostate cancer owing to the necessity of establishing a vascular network for the growth and progression of the primary and metastatic tumor. We determined whether recombinant human apolipoprotein(a) kringle V, rhLK8, produces therapeutic efficacy in an orthotopic human prostate cancer animal model. Fifty thousand androgen-independent human prostate cancer cells (PC-3MM2) were injected into the prostate of nude mice. After 3 days, these mice were randomized to receive the vehicle solution (intraperitoneally [i.p.], daily), paclitaxel (8 mg/kg i.p., weekly), rhLK8 (50 mg/kg i.p., daily), or a combination of paclitaxel and rhLK8 for 4 weeks. Treatment with paclitaxel or rhLK8 alone did not show significant therapeutic effects on tumor incidence or on tumor size compared with the control group. The combination of rhLK8 and paclitaxel significantly reduced tumor size and incidence of lymph node metastasis. Significant reduction in microvessel density and cellular proliferation and induction of apoptosis of tumor cells, and tumor-associated endothelial cells, were also achieved. Similarly, PC-3MM2 tumors growing in the tibia showed significant suppression of tumor growth and lymph node metastasis by the combination treatment with rhLK8 and paclitaxel. The integrity of the bone was significantly preserved, and apoptosis of tumor cells and tumor-associated endothelial cells was increased. In conclusion, these results suggest that targeting the tumor microenvironment with the antivascular effect of rhLK8 combined with conventional cytotoxic chemotherapy could be a new and effective approach in the treatment of androgen-independent prostate cancer and their metastases.

Neoplasia (2012) 14, 335–343

Abbreviations: Apo(a), apolipoprotein(a); GRP78, glucose-regulated protein 78; IHC, immunohistochemistry; i.p., intraperitoneal; MVD, mean vessel density; PCNA, proliferating cell nuclear antigen; PK5, plasminogen kringle 5; TUNEL, deoxynucleotidyl transferase-mediated nick end labeling

Address all correspondence to: Jang-Seong Kim, PhD, Cancer Biology Team, Mogam Biotechnology Research Institute, 341 Bojeong-dong, Giheung-gu, Yongin 446-799, Republic of Korea. E-mail: jangskim@paran.com; or Sun Jin Kim, MD, PhD, Department of Cancer Biology, The University of Texas MD Anderson Cancer Center, 1515 Holcombe Blvd, Houston, TX 77030. E-mail: sunkim@mdanderson.org

[1]This study was supported financially in part by a grant from the Korea Health 21 R&D Project, Ministry for Health, Welfare and Family Affairs, Republic of Korea (A050905). The study sponsors had no involvement in the study design, in the collection, analysis, and interpretation of data; in the writing of the article; and in the decision to submit the article for publication. The authors have no potential conflicts of interest to disclose.
Received 17 February 2012; Revised 12 March 2012; Accepted 13 March 2012

DOI 10.1593/neo.12380

Introduction

Prostate cancer is the most commonly diagnosed cancer among men in the Western world. The lifetime risk of having microscopic evidence of prostate cancer for a 50-year-old man is 40%. Prostate cancer is a complex disease, and it displays extensive heterogeneity both genetically and morphologically [1–3]. Although prostate cancer screening using serum prostate-specific antigen has led to increased detection of early-stage prostate cancer at diagnosis, many (~24%) patients have clinical or subclinical metastatic disease, which cause devastating symptoms and require systemic therapies such as hormone ablation. However, despite an initial favorable response to the therapy [4], heterogeneity and genetic instability of tumor cells lead to the development of androgen independence; then, taxane-based chemotherapy can prolong the median survival of the patients for only limited time owing to the emergence of a multidrug-resistant clonal population. Therefore, the development of a new treatment modality for androgen-independent prostate cancer is urgently required to overcome multidrug resistance. To overcome extreme heterogeneity and genetic instability of tumor cells, targeting relatively more homogeneous and genetically stable host organ microenvironment is an emerging and popular concept.

Tumor growth and metastasis require the establishment of a new vascular network, a process known as angiogenesis, to supply nutrients and oxygen and to drain waste products from the tumor mass [5–7]. Therefore, antiangiogenic therapy that can starve the tumors has been regarded as an attractive approach to treat cancer. Currently, many of these antiangiogenic molecules are under clinical investigation as anticancer drugs and most of them have shown promising anticancer efficacy in preclinical settings [8,9].

Kringle is a protein structural motif that consists of approximately 80 amino acids with conserved rigid triple disulfide bonds [10]. Kringle domains are present in several proteins with functions of a growth factor, functions in blood coagulation, and functions in fibrinolysis (hepatocyte growth factor, prothrombin, plasminogen, urokinase, etc) and have been identified as angiogenesis inhibitors both *in vitro* and *in vivo* [11]. Human apolipoprotein(a) [apo(a)] contains multiple repeats homologous to plasminogen kringle IV, followed by a single copy of a homolog of plasminogen kringle V and an inactive copy of the protease domain (Figure 1) [12], and is a glycoprotein component of lipoprotein(a) particles [13–16]. We have demonstrated that a recombinant peptide named LK68, a fragment of human apo(a) consisting of KIV_9, KIV_{10}, and KV, inhibits angiogenesis *in vitro*, in part by abrogating the activation of extracellular signal–regulated kinases 1 and 2 in endothelial cells through a protein tyrosine phosphatase–dependent mechanism [17,18]. Surprisingly, recombinant human apo(a) kringle V, termed rhLK8, displayed an antiangiogenic activity almost equivalent to that observed for LK68. It inhibited the migration of endothelial cells *in vitro* and new capillary formation *in vivo*, in part by the down-regulation of the activation of focal adhesion kinase and the inhibition of consequent formation of actin stress fibers and focal adhesions [19]. In preclinical animal models, systemic administration of LK68 proteins, retroviral gene transfer with LK68, or adenoassociated virus–mediated gene expression of LK68 suppress the growth and metastasis of human colorectal carcinoma, lung carcinoma, or hepatocellular carcinoma [17,20–22]. However, most of these studies have been performed by using ectopic animal models wherein tumor cells were implanted subcutaneously, lacking the essential cross talk between cancer cells and the organ-specific host microenvironment [23–26]. Therefore, it is necessary to evaluate the antiangiogenic and antitumor effects of a certain drug such as rhLK8 using an orthotopically implanted tumor models that can reflect the physiologically relevant interaction of cancer cells and the host microenvironment.

In this study, we evaluated the therapeutic effects of the recombinant human apo(a) kringle V, rhLK8, alone and in combination with paclitaxel against androgen-independent human prostate cancer cells growing orthotopically in nude mice. We demonstrate that the treatment produced apoptosis of tumor-associated endothelial cells and surrounding tumor cells, leading to a significant suppression of primary tumor growth and their metastasis.

Materials and Methods

Cells and Cell Culture Methods

Androgen-independent human prostate cancer cells PC-3MM2 were maintained as monolayer cultures in minimum essential medium (Life Technologies, Grand Island, NY) supplemented with 10% fetal bovine serum, sodium pyruvate (110 μg/ml), nonessential amino acids (glycine at 7.5 mg/L, L-alanine at 8.9 mg/L, L-asparagine at 13.2 mg/L, L-aspartic acid at 13.3 mg/L, L-glutamic acid at 14.7 mg/L, L-proline at 11.5 mg/L, and L-serine at 10.5 mg/L), 4 mM L-glutamine, a two-fold concentrated vitamin solution (Life Technologies), and penicillin (100 IU/ml)–streptomycin (100 μg/ml; Flow Laboratories, Rockville, MD) in an atmosphere of 5% CO_2 and 95% air at 37°C.

rhLK8 and Paclitaxel

Saccharomyces cerevisiae BJ3501 strain was transformed by an expression vector for rhLK8, which was constructed to express rhLK8 as a fusion protein to an α factor signal sequence under the control of yeast *Gal*1 promoter and subsequently processed to be secreted into the culture medium [27]. rhLK8 proteins were purified to homogeneity from the culture supernatant of *S. cerevisiae* BJ3501 expressing rhLK8 as previously described [28]. Purified rhLK8 proteins were stored in the buffer containing 100 mM NaCl and 150 mM L-glycine (pH 4.2). Paclitaxel (Taxol; Bristol-Myers Squibb C., Princeton, NJ) was diluted in distilled water at 1 mg/ml for intraperitoneal (i.p.) injection.

Animals

Male athymic nude mice (NCI-*nu*) were purchased from the Animal Production Area of the National Cancer Institute – Frederick Cancer Research Facility. The mice were housed and maintained in specific pathogen-free conditions in facilities approved by the American Association for Accreditation of Laboratory Animal Care, which met all current regulations and standards of the US Department of Health and Human Services and the National Institutes of Health. The mice were used in accordance with institutional guidelines when they were 6 to 8 weeks old.

Establishment of Orthotopic Primary and Bone Prostate Cancer Animal Models in Nude Mice

PC-3MM2 cells were harvested from subconfluent cultures by brief exposure to 0.25% trypsin and 0.02% EDTA. Trypsinization was stopped with medium containing 10% fetal bovine serum, and the cells were washed with serum-free medium and resuspended in Ca^{2+}/Mg^{2+}–free Hank's balanced salt solution. Only suspensions consisting of single cells with more than 90% viability were used. Mice were anesthetized by i.p. injection of 0.5 mg/kg body weight Nembutal (Abbott Laboratories, North Chicago, IL). PC-3MM2 cells were injected into the prostate at a concentration of 5×10^4 cells in 50 μl as described previously [29]. Briefly, a lower midline incision

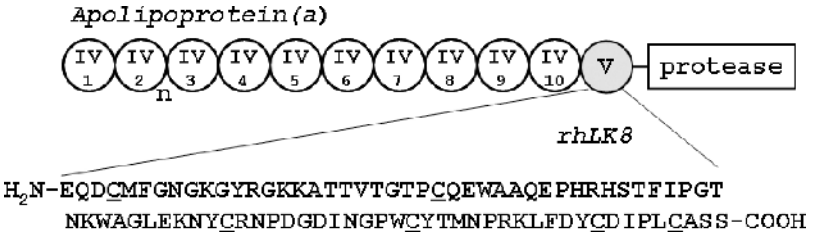

Figure 1. Schematic representation of apo(a), which contains 10 unique kringle 4-like domains (designated IV-1 through IV-10; kringle IV-2 is variably repeated), one kringle 5-like domain (KV; gray circle), and a protease domain. An 86-amino-acid sequence of the rhLK8 was shown with the cysteine residues conserved in the kringle domain underlined.

was created, and the prostate was exposed. A tumor cell suspension was injected the dorsal prostatic lobes using a 30-gauge needle. The abdominal wound was closed in one layer with wound clips (Autoclip; Clay Adams, Parsippany, NJ). To produce bone tumors, we first harvested PC-3MM2 cells as described, and before intratibial injection, the mice were anesthetized with Nembutal (0.5 mg/kg body weight). A percutaneous intraosseal injection was made by drilling a 27-gauge needle into the tibia immediately proximal to the tuberositas tibiae. After penetration of the cortical bone, the needle was further inserted into the shaft of the tibia and was used to deposit 20 μl of the tumor cell suspension (2×10^5 cells) in the cortex with the use of a calibrated, push button–controlled dispensing device (Hamilton Syringe Co, Reno, NV). To prevent leakage of cell suspensions, a cotton swab was held against the injection site for 1 minute [30,31]. The procedure was well tolerated, and there were no anesthesia-related deaths.

Therapy

In the first set of experiment, we determined the biologic optimal dose of rhLK8. Mice were injected with 5×10^4 cells of PC-3MM2 into the prostate and waited for 2 weeks to allow the tumors to develop the vascular networks essential for the tumor growth. Mice were then treated by daily i.p. injection of rhLK8 at doses of 12.5, 25, or 50 mg/kg alone or in combination with weekly i.p. injection of 8 mg/kg paclitaxel. Mice underwent necropsy 4 weeks later, and immunohistochemistry (IHC) was performed. Biologic activity of rhLK8 alone or in combination with paclitaxel was evaluated by detecting apoptosis of tumor-associated endothelial cells and surrounding tumor cells.

The second set of experiment was performed to determine the therapeutic efficacy of rhLK8 with or without paclitaxel. Three days after intraprostatic injection of cells, the mice were randomized into four groups and treated as follows: (1) daily i.p. administration of vehicle (100 mM NaCl, 150 mM L-glycine, pH 4.2), (2) i.p. injection of paclitaxel (8 mg/kg) once per week and daily i.p. injection of vehicle, (3) daily i.p. injection of rhLK8 (50 mg/kg), and (4) daily i.p. administration of rhLK8 (50 mg/kg) and i.p. injection of paclitaxel (8 mg/kg) once per week. Two weeks after intratibial injection, the mice were randomized into four groups and then treated as described previously. After 4 weeks of treatment, the mice were killed by CO_2 inhalation. Body weight, tumor incidence, tumor weight, and incidence of regional lymph node metastasis were recorded. Tumors and regional lymph nodes were processed for histologic and immunohistochemical analysis.

Digital Radiography

After 4 weeks of treatment, mice with bone tumors were anesthetized with Nembutal (0.5 mg/kg body weight) and placed in a prone position. Digital radiography of both hind limbs was carried out using the Faxitron MX-20 X-ray machine (Faxitron X-ray Corp, Wheeling, IL). Both tumor-bearing and tumor-free, uninjected control legs of each mouse were resected. Tumor weight was calculated by subtracting the weight of tumor-free leg from that of tumor-bearing leg.

Preparation of Tissues

Prostate tumor tissues or bone tumor tissues including the tibia and surrounding muscles were fixed in 10% buffered formalin and embedded in paraffin for sectioning. For frozen blocks, prostate tumor tissues were embedded immediately in ornithine carbamyl transferase compound (Miles, Elkhart, IN), snap frozen in liquid nitrogen, and stored at −70°C. Bone tumor tissues were fixed in 4% paraformaldehyde containing 0.075 M lysine and 0.01 M sodium periodate solution and embedded in ornithine carbamyl transferase compound for frozen sectioning. Fixed bone tissues were decalcified and processed as previously described [32]. All macroscopically enlarged regional lymph nodes were harvested, and the presence of metastatic disease was confirmed by hematoxylin and eosin staining.

Immunohistochemical Analyses

Paraffin embedded tissues were sectioned (4-6 μm thick) and stained for hematoxylin and eosin and proliferating cell nuclear antigen (PCNA). Frozen tissues used for CD31/platelet endothelial cell adhesion molecule 1 (PECAM-1) and/or deoxynucleotidyl transferase-mediated nick end labeling (TUNEL) staining were prepared and fixed in cold acetone. TUNEL assay was performed with a commercially available apoptosis detection kit (Promega Corp, Madison, WI) with modification. IHC procedures were performed, and all antibodies and agents for IHC were purchased from sources exactly as described previously [33]. Control samples exposed to secondary antibody alone showed no specific staining. Stained sections were examined under an Olympus BX51 microscope (Olympus, Center Valley, PA) equipped with Olympus DP71 12.5-megapixel digital microscope camera.

Immunofluorescent Double Staining for CD31/PECAM-1 (Endothelial Cells) and TUNEL

TUNEL assay was performed after CD31/PECAM-1 immunofluorescent staining as described previously [33]. For quantification of endothelial cells, the samples were incubated with 1 μg/ml of Hoechst 33342 stain for 1 minute at room temperature. Propyl gallate was placed on each slide and then covered with a glass coverslip (Fischer

Scientific, Fair Lawn, NJ). Endothelial cells were stained for red fluorescence, whereas DNA fragmentation (TUNEL assay) was stained for green fluorescence. Colocalization of red and green signals produced yellow signals (apoptotic endothelial cells).

Quantification of TUNEL, PCNA, and Mean Vessel Density

Quantification of apoptotic endothelial cells was expressed as an average of the ratio of the apoptotic endothelial cells to the total number of endothelial cells in 5 to 10 random 0.011-mm^2 fields at 400× magnification. For the quantification of total TUNEL-positive cells, the apoptotic cells were counted in 10 random 0.159-mm^2 fields at 100× magnification. To quantify PCNA-positive cells and mean vessel density (MVD), 10 to 12 random 0.159-mm^2 fields in the prostate at 100× magnification were captured for each tumor. MVD was determined according to the method described previously [33]. CD31-positive tumor vasculature was also visualized using 3,3′-diaminobenzidine (DAB) as a substrate of the horseradish peroxidase–conjugated secondary antibody. Vessel area was then determined by counting the pixel in each field using analySIS FIVE image analysis software (Olympus Soft Imaging Solutions GmbH, Münster, Germany).

Statistical Analysis

The χ^2 test was used to determine the significance of differences in tumor incidence and incidence of lymph node metastasis. Differences in tumor weight of mice were compared with Mann-Whitney *U* test. The unpaired Student's *t* test was used to evaluate the differences in PCNA-positive cells, MVD (CD31/PECAM-1), number of apoptotic cells (TUNEL), and percentage of apoptotic endothelial cells.

Results

In the first set of experiment, intermittent apoptosis of tumor-associated endothelial cells and tumor cells fed by these vessels was observed with a single treatment with paclitaxel and more so with 25 or 50 mg/kg rhLK8 alone. However, the induction of apoptosis was significantly increased with the combined treatment of rhLK8 with paclitaxel in a dose-dependent manner (data not shown) without detectable local or systemic toxicities. On the basis of these results, the optimal biologic dose of rhLK8 was determined to be 50 mg/kg.

In the next set of experiments, we determined the therapeutic effects of rhLK8 administered alone or in combination with paclitaxel against PC-3MM2 cells growing orthotopically in the prostate of nude mice. Results of the two independent experiments were similar and therefore combined for analysis (Table 1). All the control mice (15/15) developed large prostate tumors (median weight = 2.3 g, range = 0.4-3.6 g) and had histologically confirmed metastasis to the regional lymph nodes. In the paclitaxel-treated group, all 19 mice had prostate tumors (median weight = 2.0 g, range = 0.4-3.8 g) and also had lymph node metastasis. All mice administered with rhLK8 (17/17) had prostate tumors (median weight = 1.8 g, range = 0.1-3.1 g), and 12 of 17 mice had lymph node metastasis. Mice treated with the combination of rhLK8 and paclitaxel showed significantly decreased tumor weight (median weight = 0.6 g, range = 0-2.6 g, $P < .01$, compared with the control group) and lymph node metastasis (10/18, $P < .01$, compared with the control group). Tumor incidence was also decreased but not statistically significant.

Table 1. Treatment of PC-3MM2 Implanted into the Prostate of Male Nude Mice with rhLK8 and Paclitaxel.

Treatment Groups	Incidence of Tumor	Tumor Weight (g), Median (Range)	Incidence of L/N Metastasis
Vehicle	15/15	2.3 (0.4-3.6)	15/15
Paclitaxel	19/19	2.0 (0.4-3.8)	19/19
rhLK8	17/17	1.8 (0.1-3.1)	12/17
rhLK8 + paclitaxel	15/18	0.6 (0-2.6)*	10/18*

A total of 5×10^4 PC-3MM2 cells were implanted into the prostate of nude mice. Three days later, treatment with vehicle, paclitaxel (8 mg/kg, weekly i.p. injection), or rhLK8 (50 mg/kg, daily i.p. injection), alone or in combination with paclitaxel, was started and continued for 4 weeks.
*$P < .01$.

Cell Proliferation and Apoptosis

IHC analyses were carried out at the peripheral zones of the tumors to avoid zones of central necrosis. We determined whether the decrease in tumor weight and lymph node metastasis in mice treated with rhLK8 alone or in combination with paclitaxel was due to the inhibition of tumor cell proliferation, the induction of tumor cell apoptosis, or both. The number of PCNA-positive and TUNEL-positive cells in PC-3MM2 tumors was counted (Figure 2 and Table 2). The mean number of PCNA-positive tumor cells in tumors from control mice was 197.8 ± 15.5. Administration of rhLK8 did not significantly decrease the number of proliferating cells (187.1 ± 10.3, $P > .05$). However, tumors from mice treated with paclitaxel or paclitaxel plus rhLK8 showed a significant decrease in the number of PCNA-positive cells (151.4 ± 11.2 and 150.5 ± 14.4, respectively, $P < .005$). The mean number of TUNEL-positive tumor cells in tumors from control mice and mice treated with paclitaxel had similar levels of apoptosis (5.2 ± 4.8 and 3.9 ± 5.9, respectively, $P > .05$). Administration of rhLK8 slightly increased the number of apoptotic tumor cells, but there was no statistical significance (11.4 ± 13.3, $P > .05$). However, in mice treated with rhLK8 in combination with paclitaxel, there was a significant increase in the number of TUNEL-positive tumor cells (29.5 ± 13.4, $P < .01$).

Microvessel Density

Next, we determined whether the increase in apoptosis of tumor cells correlated with a suppression of vascularization. Samples were stained for CD31/PECAM-1 to determine MVD. In control tumors, the MVD was 32.7 ± 9.3. Treatment with paclitaxel or rhLK8 did not decrease the MVD (36.3 ± 15.2 and 28.8 ± 12.8, respectively, $P > .05$), whereas treatment with rhLK8 in combination with paclitaxel produced a significant decrease in MVD (16.9 ± 10.4, $P < .01$; Table 2). We also determined the vessel area by counting the pixels generated by CD31-positive tumor vasculature. Consistent with the result of MVD analysis, the relative vessel area in tumors from control mice (3.7 ± 1.2) was similar to that observed in tumors from mice treated with paclitaxel or rhLK8 (4.0 ± 1.5 and 3.4 ± 2.3, respectively, $P > .05$), whereas treatment with rhLK8 plus paclitaxel decreased significantly the relative vessel area (1.8 ± 0.8, $P < .01$; Figure 2).

Immunofluorescent Double Staining for Endothelial Cells (CD31/PECAM-1) and TUNEL

We also determined whether the treatment with paclitaxel, rhLK8, or rhLK8 plus paclitaxel can induce the apoptosis of tumor-associated endothelial cells. The immunofluorescent double staining for CD31 (*red*) and TUNEL (*green*) and subsequent colocalization technique allowed detection of apoptotic tumor cells (*green*) and apoptotic tumor-associated endothelial cells (*yellow*; Figure 3 and Table 2). In the control group and the paclitaxel-treated group, the median ratio of apoptotic

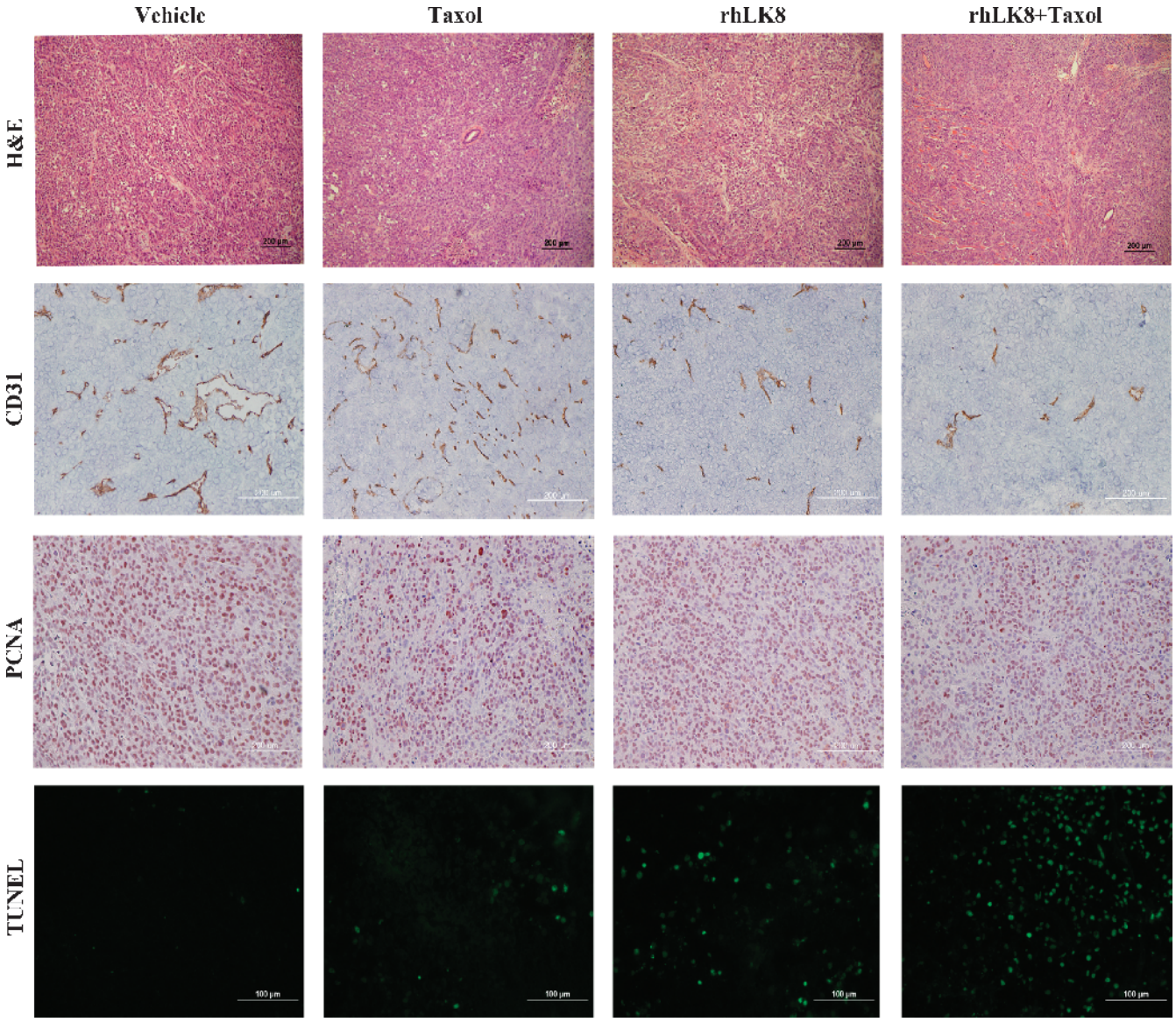

Figure 2. Analysis of cell proliferation, apoptosis, and MVD. Prostate tumor specimens from different treatment groups underwent immunohistochemical analysis for the expression of CD31 (MVD), PCNA (cell proliferation), and apoptosis (TUNEL). Treatment of PC-3MM2 human prostate cancer in nude mice with rhLK8 plus paclitaxel significantly decreased MVD and tumor cell proliferation and increased apoptotic tumor cells.

endothelial cells was 0% (range = 0-5% and 0-7%, respectively). Treatment with rhLK8 significantly increased the ratio of apoptotic endothelial cells (median = 6%, range = 0%-14%, $P < .005$) and more so with the combination of rhLK8 and paclitaxel (median = 23%, range = 0%-29%, $P < .01$). The differences in the ratio of apoptotic endothelial cells between tumors from mice treated with rhLK8 and mice treated with rhLK8 plus paclitaxel were also significant ($P < .05$).

Therapy for Nude Mice Bearing PC-3MM2 Tumors in the Tibia

We determined whether the biologic activity of rhLK8 observed in prostate tumors growing in the prostate of nude mice can be extrapolated to the prostate tumors growing in the tibia of nude mice. We injected the PC-3MM2 human prostate carcinoma cells into the tibia of nude mice and waited for 2 weeks to allow the tumors to develop

Table 2. Response to Treatment of Human Prostate Carcinoma (PC-3MM2) Growing in the Prostate of Nude Mice.

Treatment Groups*	Tumor Cells		Endothelial Cells	
	PCNA[+†]	TUNEL[+†]	CD31[+†]	CD31/TUNEL[+‡] (%)
Vehicle	197.8 ± 15.5	5.2 ± 4.8	32.7 ± 9.3	0 (0-5)
Paclitaxel	151.4 ± 11.2[§]	3.9 ± 5.9	36.3 ± 15.2	0 (0-7)
rhLK8	187.1 ± 10.3	11.4 ± 13.3	28.8 ± 12.8	6 (0-14)[§]
rhLK8 + paclitaxel	150.5 ± 14.4[§]	29.5 ± 13.4[¶]	16.9 ± 10.4[¶]	23 (0-29)[¶]

*A total of 5×10^4 PC-3MM2 cells were implanted into the prostate of nude mice. Three days later, treatment with vehicle, paclitaxel (8 mg/kg, weekly i.p. injection), or rhLK8 (50 mg/kg, daily i.p. injection), alone or in combination with paclitaxel, was started and continued for 4 weeks.
†Mean ± SD.
‡Ratio of the median number of apoptotic endothelial cells to the total number of endothelial cells in 7 to 10 random 0.159-mm^2 fields.
§$P < .005$.
¶$P < .01$.

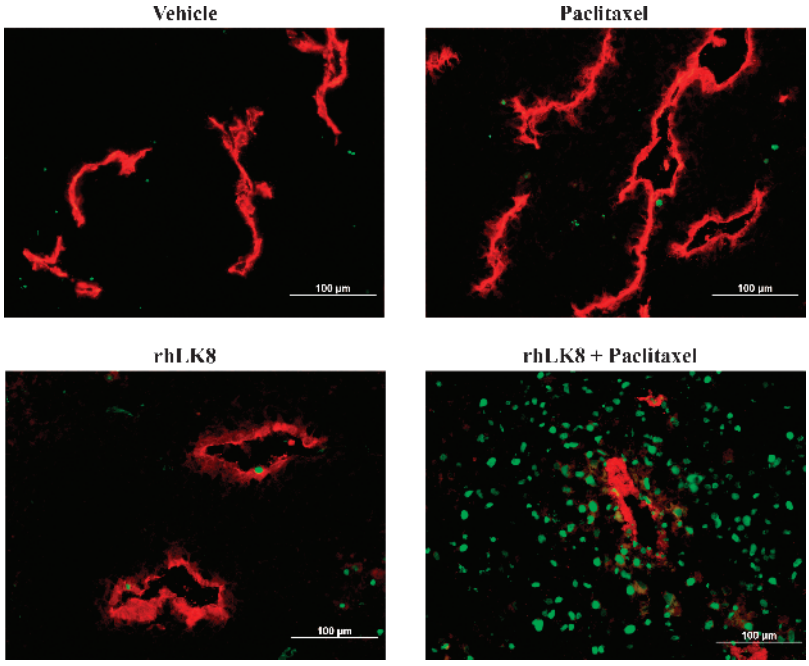

Figure 3. Double immunofluorescence staining of prostate tumor specimens for CD31/PECAM-1 (red) and TUNEL (green). Note the significant increase of apoptosis of tumor-associated endothelial cells as well as adjacent tumor cells in the prostate tumors treated with rhLK8 plus paclitaxel.

vascular networks essential for the tumor growth. Then we treated mice with rhLK8 alone or in combination with paclitaxel for 4 weeks. All mice had tumors in their legs and also had regional lymph node metastasis. Mice from the control group had large tumors in the tibia and surrounding muscles (median = 1.2 g, range = 0.5-2.0 g). Median tumor sizes of mice treated with paclitaxel or rhLK8 were 0.8 g (range = 0.8-1.5 and 0.2-4.3 g, respectively, $P > .05$, compared with the control group). However, treatment with rhLK8 in combination with paclitaxel produced a significant therapeutic efficacy on tumor size (median = 0.6 g, range = 0.2-1.4 g, $P < .05$, compared with the control group) (Table 3).

As shown in Figure 4*A*, digital radiography of the hind legs revealed severe destruction of bone in the control group of mice or in the mice treated with paclitaxel. Osteolytic bone lesions were less severe with the treatment with rhLK8 and were the least severe with the combination treatment with rhLK8 and paclitaxel. In mice treated with rhLK8 and paclitaxel, bone integrity was well preserved.

We also determined whether the results produced by the treatment with rhLK8 in combination with paclitaxel resulted from the induction of apoptosis in tumor-associated endothelial cells and the surrounding tumor cells. Tumor specimens were stained for CD31/PECAM-1 (red) and TUNEL (green) to detect apoptotic (TUNEL positive) tumor cells (green) and apoptotic endothelial cells (yellow). Tumor specimens from control mice or from mice treated with paclitaxel showed little apoptotic tumor cells and tumor-associated endothelial cells. However, treatment with rhLK8 induced apoptosis of tumor cells and tumor-associated endothelial cells, and this induction of apoptosis was significantly increased with the combined treatment with rhLK8 and paclitaxel (Figure 4*B*).

Discussion

The standard therapy for men with hormone-refractory prostate cancer is taxane-based chemotherapy. However, responses are not durable, and progression of disease is frequent. Therefore, there is an unmet medical need for the alternative therapeutic approaches that can improve the prognosis of patients.

Tumor-Associated Endothelial Cells

It has been reported that the blood vessels in the tumors are irregular, tortuous, and leaky than those of normal blood vessels [7,34]. Endothelial cells in the human tumors are highly proliferative than those in their corresponding normal tissues. Although prostate carcinoma has a relatively low endothelial cell proliferative index, endothelial cell turnover in the prostate carcinoma (mean ± SD = 2.0% ± 1.4%; median = 1.9%) is ~20-fold higher than the proliferative cell index of the endothelial cells (around 0.1%) in the normal tissues [35]. Given the findings that antiangiogenic agents may target the proliferating endothelial cells but not the dormant endothelial cells, this selectivity should lead to the minimal adverse effects even after prolonged treatment. Furthermore, targeting of endothelial cells may have a self-amplification mechanism in that the induction of apoptosis in endothelial cells may lead to the apoptosis in ~70-fold more tumor cells dependent on those endothelial cells, as assessed by the findings that

Table 3. Treatment of PC-3MM2 Implanted into the Tibia of Male Nude Mice with rhLK8 and Paclitaxel.

Treatment Groups	Incidence of Tumor	Tumor Weight (g), Median (Range)	Incidence of L/N Metastasis
Vehicle	10/10	1.2 (0.5-2.0)	10/10
Paclitaxel	8/8	0.8 (0.5-1.8)	8/8
rhLK8	8/8	0.8 (0.2-4.3)	8/8
rhLK8 + paclitaxel	10/10	0.6 (0.2-1.4)*	10/10

A total of 2×10^5 PC-3MM2 cells were implanted into the tibia of nude mice. Two weeks later, treatment with vehicle, paclitaxel (8 mg/kg, weekly i.p. injection), or rhLK8 (50 mg/kg, daily i.p. injection), alone or in combination with paclitaxel, was started and continued for 4 weeks.
*$P < .05$.

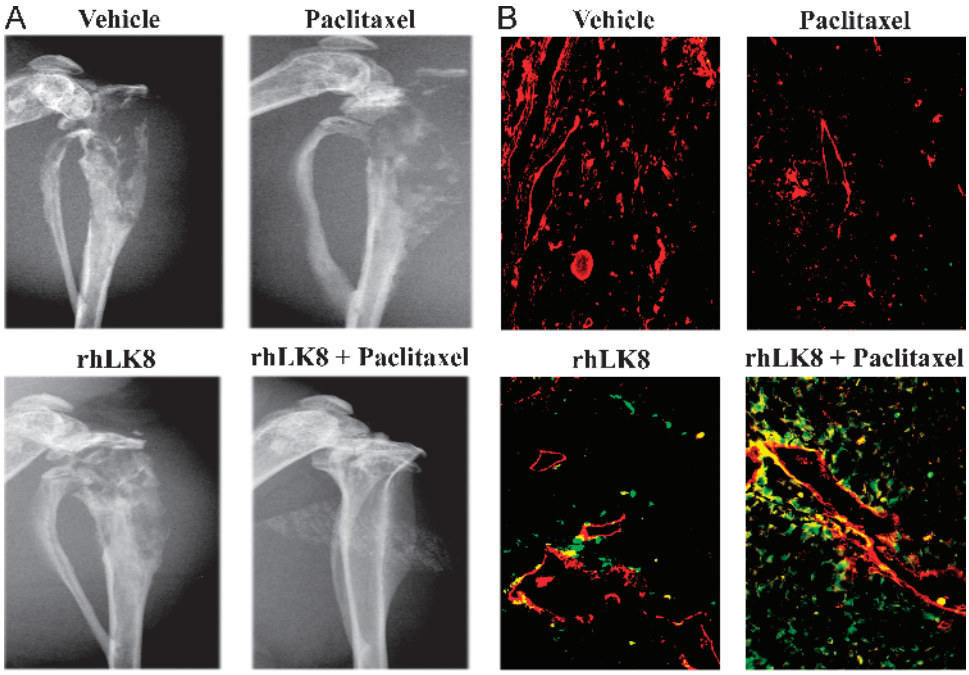

Figure 4. Digital radiography and immunofluorescent double labeling of tumors derived from human prostate cancer cells growing in the tibia of nude mice for CD31/PECAM-1 and TUNEL. (A) Digital radiography of the hind legs revealed destruction of bone in control mice or in mice treated with paclitaxel. Mice treated rhLK8 alone had diminished bone lysis, and the combination of rhLK8 with paclitaxel was associated with preservation of the bone structure, in a dose-dependent manner. (B) Tumor specimens from control mice or mice treated with paclitaxel showed little apoptotic tumor cells and tumor-associated endothelial cells. However, treatment with rhLK8 induced apoptosis of tumor cells and tumor-associated endothelial cells, and this induction of apoptosis was significantly increased with the combined treatment with rhLK8 and paclitaxel.

an index of overall ratio of proliferating tumor cells to the proliferating endothelial cells in the human prostate carcinoma has been determined to be between 40 and 70 [35]. Microvessel density has been considered as a negative prognostic indicator for prostate cancer [36], with a significant correlation among Gleason score, pathologic stage, tumor metastasis, and patient survival [37,38]. Therefore, targeting angiogenesis has been regarded as a promising new treatment for prostate cancer, and this has been supported by several clinical trials of the docetaxel-based combination with angiogenesis inhibitors [39].

Therapeutic Efficacy

In the present study, treatment with paclitaxel alone significantly decreased the proliferation index of tumor cells but did not affect tumor-associated endothelial cells. Nevertheless, treatment with rhLK8 alone induced the apoptosis of endothelial cells but did not affect the proliferation of tumor cells. Significantly, combined treatment with rhLK8 and paclitaxel decreased cellular proliferation index with a significant induction of apoptosis of endothelial cells of tumor-associated vasculature, which implicated a potential synergistic therapeutic effect of rhLK8 combined with paclitaxel. Moreover, induction of apoptosis of tumor cells was also significantly increased, suggesting that apoptosis of endothelial cells may lead to the disruption of tumor vasculature followed by necrosis of surrounding tumors. As previously reported, antiangiogenic therapy is often not cytocidal but cytostatic in nature; the treatment outcome of antiangiogenic drugs as a single agent is relatively limited but a combination of antiangiogenic drugs with conventional chemotherapy may enhance treatment outcomes [40,41], although the underlying mechanism of this synergism is not yet clear. A potential explanation can be referred to the inherent leakiness of the tumor vasculature and, hence, the impairment of drug delivery to cancer cells that is caused by a high interstitial pressure; antiangiogenic therapy might initially make blood flow more efficient, resulting in improved tissue oxygenation and increased delivery of cytotoxic agents [42–44].

Apolipoprotein(a)

Plasminogen kringle 5 (PK5), which showed a significant sequence identity with apo(a) kringle V, has the most potent antiangiogenic activities to inhibit the growth of a variety of tumors in animal models with the significantly decreased mean microvessel density [45–50]. It inhibits the proliferation, migration, and tube formation of endothelial cells *in vitro* [51,52] and induces cell cycle arrest [53], autophagy [54], and apoptosis of proliferating endothelial cells [55]. PK5 interacts with a chaperone protein associated with stress in endoplasmic reticulum, the glucose-regulated protein 78 (GRP78), on the cell surface of the proliferating endothelial cells [55]. GRP78–caspase 7 complex is believed to prevent the cells from apoptotic cell death. Binding of PK5 with GRP78 may cause the dissociation of this complex, subsequent release, and activation of caspase 7, leading to the apoptotic cell death. Taken together with the findings that PK5 treatment promotes mitochondrial depolarization, followed by the release of cytochrome *c* and activation of caspase cascades including caspase 3, 6, and 7 [50], PK5 seems to induce the apoptosis in endothelial cells through the intrinsic pathway. Binding of PK5 to another cell surface target, the voltage-dependent anion channel, and induction of apoptosis through this interaction have also been reported [56]. These studies have also shown

that PK5 can induce the apoptosis of tumor cells under stress, such as hypoxia, in addition to the endothelial cells. Although we have clearly demonstrated the induction of apoptosis mediated by rhLK8 in endothelial cells of the tumor-associated vasculature in this study, its direct effect on endothelial cell *in vitro* is moderate and much remains to be elucidated. Unlike PK5, rhLK8 did not induce the apoptosis of any tumor cells tested *in vitro*. However, under a limited condition such as nutrient deprivation, treatment with rhLK8 showed induction of endothelial cell apoptosis *in vitro*. Moreover, our preliminary data showed that rhLK8 may induce apoptosis of endothelial cells *in vitro* through binding with the GRP78 protein on the endothelial cell surface. No rhLK8-mediated activation of caspase 3 was observed in endothelial cells, when the expression of GRP78 had been knocked down by the transduction of GRP78 siRNA (J.H. Ahn et al., unpublished data). However, this does not rule out the possibility that rhLK8 may affect the interaction of tumor-associated vasculatures with tumor cells or other cells such as immune cells *in vivo* because PK5 can exert its antitumor activity either by inhibiting the recruitment of tumor-associated macrophages or by promoting the recruitment of neutrophils or NKT lymphocytes [45,47]. The potential direct effects of rhLK8 on the growth of tumors remain largely to be elucidated, although LK8 gene expression in the hepatocellular carcinoma cells inhibited primary tumor growth and prolonged survival [22].

We have demonstrated here that administration of rhLK8 in combination with paclitaxel can produce a significant therapy against androgen-independent human prostate carcinoma cells growing orthotopically in the prostate of nude mice. Moreover, the combination therapy for rhLK8 with paclitaxel significantly inhibited the growth of prostate tumor cells in the tibial bone of nude mice, leaving bone integrity of these mice well preserved.

In conclusion, these results suggest that targeting the tumor microenvironment with the antivascular activity of rhLK8 combined with conventional cytotoxic chemotherapy could be a new and effective approach in the treatment of androgen-independent prostate cancer and their metastases.

References

[1] DeMarzo AM, Nelson WG, Isaacs WB, and Epstein JI (2003). Pathological and molecular aspects of prostate cancer. *Lancet* **361**, 955–964.

[2] Roy-Burman P, Zheng J, and Miller GJ (1997). Molecular heterogeneity in prostate cancer: can *TP53* mutation unravel tumorigenesis? *Mol Med Today* **3**, 476–482.

[3] Dai B, Kim O, Xie Y, Guo Z, Xu K, Wang B, Kong X, Melamed J, Chen H, Bieberich CJ, et al. (2006). Tyrosine kinase Etk/BMX is up-regulated in human prostate cancer and its overexpression induces prostate intraepithelial neoplasia in mouse. *Cancer Res* **66**, 8058–8064.

[4] Smith PC, Hobisch A, Lin DL, Culig Z, and Keller ET (2001). Interleukin-6 and prostate cancer progression. *Cytokine Growth Factor Rev* **12**, 33–40.

[5] Folkman J (1971). Tumor angiogenesis: therapeutic implications. *N Engl J Med* **285**, 1182–1186.

[6] Folkman J (1995). Angiogenesis in cancer, vascular, rheumatoid and other disease. *Nat Med* **1**, 27–31.

[7] Carmeliet P and Jain RK (2000). Angiogenesis in cancer and other diseases. *Nature* **407**, 249–257.

[8] Folkman J (2007). Angiogenesis: an organizing principle for drug discovery? *Nat Rev Drug Discov* **6**, 273–286.

[9] Mauriz JL and Gonzalez-Gallego J (2008). Antiangiogenic drugs: current knowledge and new approaches to cancer therapy. *J Pharm Sci* **97**, 4129–4154.

[10] Patthy L, Trexler M, Vali Z, Banyai L, and Varadi A (1984). Kringles: modules specialized for protein binding. Homology of the gelatin-binding region of fibronectin with the kringle structures of proteases. *FEBS Lett* **171**, 131–136.

[11] Cao Y, Cao R, and Veitonmaki N (2002). Kringle structures and antiangiogenesis. *Curr Med Chem Anticancer Agents* **2**, 667–681.

[12] McLean JW, Tomlinson JE, Kuang WJ, Eaton DL, Chen EY, Fless GM, Scanu AM, and Lawn RM (1987). cDNA sequence of human apolipoprotein(a) is homologous to plasminogen. *Nature* **330**, 132–137.

[13] Guevara J Jr, Knapp RD, Honda S, Northup SR, and Morrisett JD (1992). A structural assessment of the apo[a] protein of human lipoprotein[a]. *Proteins* **12**, 188–199.

[14] Kraft HG, Lingenhel A, Pang RW, Delport R, Trommsdorff M, Vermaak H, Janus ED, and Utermann G (1996). Frequency distributions of apolipoprotein(a) kringle IV repeat alleles and their effects on lipoprotein(a) levels in Caucasian, Asian, and African populations: the distribution of null alleles is non-random. *Eur J Hum Genet* **4**, 74–87.

[15] Fless GM, ZumMallen ME, and Scanu AM (1986). Physicochemical properties of apolipoprotein(a) and lipoprotein(a-) derived from the dissociation of human plasma lipoprotein (a). *J Biol Chem* **261**, 8712–8718.

[16] Callow MJ and Rubin EM (1995). Site-specific mutagenesis demonstrates that cysteine 4326 of apolipoprotein B is required for covalent linkage with apolipoprotein (a) *in vivo*. *J Biol Chem* **270**, 23914–23917.

[17] Kim JS, Chang JH, Yu HK, Ahn JH, Yum JS, Lee SK, Jung KH, Park DH, Yoon Y, Byun SM, et al. (2003). Inhibition of angiogenesis and angiogenesis-dependent tumor growth by the cryptic kringle fragments of human apolipoprotein(a). *J Biol Chem* **278**, 29000–29008.

[18] Ahn JH, Kim JS, Yu HK, Lee HJ, and Yoon Y (2004). A truncated kringle domain of human apolipoprotein(a) inhibits the activation of extracellular signal–regulated kinase 1 and 2 through a tyrosine phosphatase–dependent pathway. *J Biol Chem* **279**, 21808–21814.

[19] Kim JS, Yu HK, Ahn JH, Lee HJ, Hong SW, Jung KH, Chang SI, Hong YK, Joe YA, Byun SM, et al. (2004). Human apolipoprotein(a) kringle V inhibits angiogenesis *in vitro* and *in vivo* by interfering with the activation of focal adhesion kinases. *Biochem Biophys Res Commun* **313**, 534–540.

[20] Yu HK, Kim JS, Lee HJ, Ahn JH, Lee SK, Hong SW, and Yoon Y (2004). Suppression of colorectal cancer liver metastasis and extension of survival by expression of apolipoprotein(a) kringles. *Cancer Res* **64**, 7092–7098.

[21] Yu HK, Ahn JH, Lee HJ, Lee SK, Hong SW, Yoon Y, and Kim JS (2005). Expression of human apolipoprotein(a) kringles in colon cancer cells suppresses angiogenesis-dependent tumor growth and peritoneal dissemination. *J Gene Med* **7**, 39–49.

[22] Lee K, Yun ST, Kim YG, Yoon Y, and Jo EC (2006). Adeno-associated virus-mediated expression of apolipoprotein (a) kringles suppresses hepatocellular carcinoma growth in mice. *Hepatology* **43**, 1063–1073.

[23] Fidler IJ, Kim SJ, and Langley RR (2007). The role of the organ microenvironment in the biology and therapy of cancer metastasis. *J Cell Biochem* **101**, 927–936.

[24] McCabe NP, Kerr BA, Madajka M, Vasanji A, and Byzova TV (2011). Augmented osteolysis in SPARC-deficient mice with bone-residing prostate cancer. *Neoplasia* **13**, 31–39.

[25] Zhang J, Sud S, Mizutani K, Gyetko MR, and Pienta KJ (2011). Activation of urokinase plasminogen activator and its receptor axis is essential for macrophage infiltration in a prostate cancer mouse model. *Neoplasia* **13**, 23–30.

[26] Wittig-Blaich SM, Kacprzyk LA, Eismann T, Bewerunge-Hudler M, Kruse P, Winkler E, Strauss WS, Hibst R, Steiner R, Schrader M, et al. (2011). Matrix-dependent regulation of AKT in Hepsin-overexpressing PC3 prostate cancer cells. *Neoplasia* **13**, 579–589.

[27] Lee TH, Kim MD, Shin SY, Lim HK, and Seo JH (2006). Disruption of hexokinase II (HXK2) partly relieves glucose repression to enhance production of human kringle fragment in gratuitous recombinant *Saccharomyces cerevisiae*. *J Biotechnol* **126**, 562–567.

[28] Kang KY, Park JH, Lim IH, Kim SG, Park SH, Kim WK, Hong JW, You HK, Jung KH, and Kim CW (2006). Crystallization of antiangiogenic Kringle V derived from human apolipoprotein A: crystallization applied to purification and formulation. *Biosci Biotechnol Biochem* **70**, 916–925.

[29] Yazici S, Kim SJ, Busby JE, He J, Thaker P, Yokoi K, Fan D, and Fidler IJ (2005). Dual inhibition of the epidermal growth factor and vascular endothelial growth factor phosphorylation for antivascular therapy of human prostate cancer in the prostate of nude mice. *Prostate* **65**, 203–215.

[30] Kim SJ, Uehara H, Karashima T, Shepherd DL, Killion JJ, and Fidler IJ (2003). Blockade of epidermal growth factor receptor signaling in tumor cells and tumor-associated endothelial cells for therapy of androgen-independent human prostate cancer growing in the bone of nude mice. *Clin Cancer Res* **9**, 1200–1210.

[31] Uehara H, Kim SJ, Karashima T, Shepherd DL, Fan D, Tsan R, Killion JJ, Logothetis C, Mathew P, and Fidler IJ (2003). Effects of blocking platelet-derived growth factor-receptor signaling in a mouse model of experimental prostate cancer bone metastases. *J Natl Cancer Inst* **95**, 458–470.

[32] Mori S, Sawai T, Teshima T, and Kyogoku M (1988). A new decalcifying technique for immunohistochemical studies of calcified tissue, especially applicable to cell surface marker demonstration. *J Histochem Cytochem* **36**, 111–114.

[33] Kim SJ, Uehara H, Yazici S, Langley RR, He J, Tsan R, Fan D, Killion JJ, and Fidler IJ (2004). Simultaneous blockade of platelet-derived growth factor-receptor and epidermal growth factor-receptor signaling and systemic administration of paclitaxel as therapy for human prostate cancer metastasis in bone of nude mice. *Cancer Res* **64**, 4201–4208.

[34] Baish JW and Jain RK (2000). Fractals and cancer. *Cancer Res* **60**, 3683–3688.

[35] Eberhard A, Kahlert S, Goede V, Hemmerlein B, Plate KH, and Augustin HG (2000). Heterogeneity of angiogenesis and blood vessel maturation in human tumors: implications for antiangiogenic tumor therapies. *Cancer Res* **60**, 1388–1393.

[36] Weidner N, Carroll PR, Flax J, Blumenfeld W, and Folkman J (1993). Tumor angiogenesis correlates with metastasis in invasive prostate carcinoma. *Am J Pathol* **143**, 401–409.

[37] Borre M, Offersen BV, Nerstrom B, and Overgaard J (1998). Microvessel density predicts survival in prostate cancer patients subjected to watchful waiting. *Br J Cancer* **78**, 940–944.

[38] Bono AV, Celato N, Cova V, Salvadore M, Chinetti S, and Novario R (2002). Microvessel density in prostate carcinoma. *Prostate Cancer Prostatic Dis* **5**, 123–127.

[39] Aragon-Ching JB and Dahut WL (2008). The role of angiogenesis inhibitors in prostate cancer. *Cancer J* **14**, 20–25.

[40] Gerber HP and Ferrara N (2005). Pharmacology and pharmacodynamics of bevacizumab as monotherapy or in combination with cytotoxic therapy in preclinical studies. *Cancer Res* **65**, 671–680.

[41] Canu B, Fioravanti A, Orlandi P, Di Desidero T, Ali G, Fontanini G, Di Paolo A, Del Tacca M, Danesi R, and Bocci G (2011). Irinotecan synergistically enhances the antiproliferative and proapoptotic effects of axitinib *in vitro* and improves its anticancer activity *in vivo*. *Neoplasia* **13**, 217–229.

[42] Jain RK (2005). Normalization of tumor vasculature: an emerging concept in antiangiogenic therapy. *Science* **307**, 58–62.

[43] Ma J and Waxman DJ (2008). Combination of antiangiogenesis with chemotherapy for more effective cancer treatment. *Mol Cancer Ther* **7**, 3670–3684.

[44] Huang G and Chen L (2008). Tumor vasculature and microenvironment normalization: a possible mechanism of antiangiogenesis therapy. *Cancer Biother Radiopharm* **23**, 661–667.

[45] Perri SR, Nalbantoglu J, Annabi B, Koty Z, Lejeune L, Francois M, Di Falco MR, Beliveau R, and Galipeau J (2005). Plasminogen kringle 5–engineered glioma cells block migration of tumor-associated macrophages and suppress tumor vascularization and progression. *Cancer Res* **65**, 8359–8365.

[46] Yang X, Cheng R, Li C, Cai W, Ma JX, Liu Q, Yang Z, Song Z, Liu Z, and Gao G (2006). Kringle 5 of human plasminogen suppresses hepatocellular carcinoma growth both in grafted and xenografted mice by anti-angiogenic activity. *Cancer Biol Ther* **5**, 399–405.

[47] Perri SR, Martineau D, Francois M, Lejeune L, Bisson L, Durocher Y, and Galipeau J (2007). Plasminogen Kringle 5 blocks tumor progression by anti-angiogenic and proinflammatory pathways. *Mol Cancer Ther* **6**, 441–449.

[48] Jin GH, Ma DY, Wu N, Marikar FM, Jin SZ, Jiang WW, Liu Y, and Hua ZC (2007). Combination of human plasminogen kringle 5 with ionizing radiation significantly enhances the efficacy of antitumor effect. *Int J Cancer* **121**, 2539–2546.

[49] Fan JK, Xiao T, Gu JF, Wei N, He LF, Ding M, and Liu XY (2008). Increased suppression of oncolytic adenovirus carrying mutant k5 on colorectal tumor. *Biochem Biophys Res Commun* **374**, 198–203.

[50] Li Y, Han W, Zhang Y, Yuan L, Shi X, Yu Y, and Wang J (2008). Intramuscular electroporation of a plasmid encoding human plasminogen kringle 5 induces growth inhibition of Lewis lung carcinoma in mice. *Cancer Biother Radiopharm* **23**, 332–341.

[51] Cao Y, Chen A, An SS, Ji RW, Davidson D, and Llinas M (1997). Kringle 5 of plasminogen is a novel inhibitor of endothelial cell growth. *J Biol Chem* **272**, 22924–22928.

[52] Ji WR, Barrientos LG, Llinas M, Gray H, Villarreal X, DeFord ME, Castellino FJ, Kramer RA, and Trail PA (1998). Selective inhibition by kringle 5 of human plasminogen on endothelial cell migration, an important process in angiogenesis. *Biochem Biophys Res Commun* **247**, 414–419.

[53] Lu H, Dhanabal M, Volk R, Waterman MJ, Ramchandran R, Knebelmann B, Segal M, and Sukhatme VP (1999). Kringle 5 causes cell cycle arrest and apoptosis of endothelial cells. *Biochem Biophys Res Commun* **258**, 668–673.

[54] Nguyen TM, Subramanian IV, Kelekar A, and Ramakrishnan S (2007). Kringle 5 of human plasminogen, an angiogenesis inhibitor, induces both autophagy and apoptotic death in endothelial cells. *Blood* **109**, 4793–4802.

[55] Davidson DJ, Haskell C, Majest S, Kherzai A, Egan DA, Walter KA, Schneider A, Gubbins EF, Solomon L, Chen Z, et al. (2005). Kringle 5 of human plasminogen induces apoptosis of endothelial and tumor cells through surface-expressed glucose-regulated protein 78. *Cancer Res* **65**, 4663–4672.

[56] Gonzalez-Gronow M, Kaczowka SJ, Payne S, Wang F, Gawdi G, and Pizzo SV (2007). Plasminogen structural domains exhibit different functions when associated with cell surface GRP78 or the voltage-dependent anion channel. *J Biol Chem* **282**, 32811–32820.